Antifungal Azoles by Transition Metal Coordination

Subjects: Chemistry, Medicinal

Contributor: Youri Cortat , Fabio Zobi

Coordination compounds featuring one or more antifungal azole (AA) ligands constitute an interesting family of candidate molecules, given their medicinal polyvalence and the viability of drug complexation as a strategy to improve and repurpose available medications.

repurposing antifungal azole metal

1. Introduction

The lack of new medically active molecules remains an issue for the treatment of several diseases and infections. In particular, cancer is responsible for approximately one death in six worldwide, and its incidence will probably raise from 18.1 million cases in 2018 to 29.4 million in 2040, according to the World Health Organization report on cancer of 2020 [1]. At the same time, antimicrobial resistance (AMR) poses a serious threat to global health, possibly causing 10 million death a year by 2050 if no efficient measures are rapidly taken [2]. Indeed, the last class of antibiotics was discovered more than 30 years ago. Since then, big pharmaceutical companies have scarcely invested in the development of new antibiotics due to an absence of financial interest [3]. Moreover, pathogens of the bacteria, fungi and protozoa groups known for developing AMR are responsible for certain neglected tropical diseases (NTDs), which are causing devastating human and material consequences in developing countries. Namely, NTDs are estimated to affect 1.7 billion people, causing 200,000 deaths each year [4].

Antifungal azoles (AAs, Scheme 1) form a class of therapeutic compounds that display selective activity against fungal pathogens by blocking ergosterol biosynthesis through the inhibition of lanosterol C_{14}-demethylation (**Figure 1**A). This process occurs via coordination to the iron heme porphyrin moiety of the CYP51 enzyme (**Figure 1**B), which makes it impossible to perform an oxidative removal of the lanosterol methyl group [5][6][7]. As a consequence, the fungal organism experiences sterol depletion and accumulation of derivatives that are unable to orientate correctly within the phospholipid bilayer, ultimately leading to loss of membrane integrity and cell lysis [8][9]. Although concomitant binding to human enzymes can cause serious side effects [10], careful tuning of the drug structure and recognition of the medically relevant moieties through structure–activity relationship (SAR) studies have enabled the design of more viable generations of AAs. The resulting selectivity is quite remarkable, considering the higher similarity between humans and fungi compared to prokaryotic parasites [11].

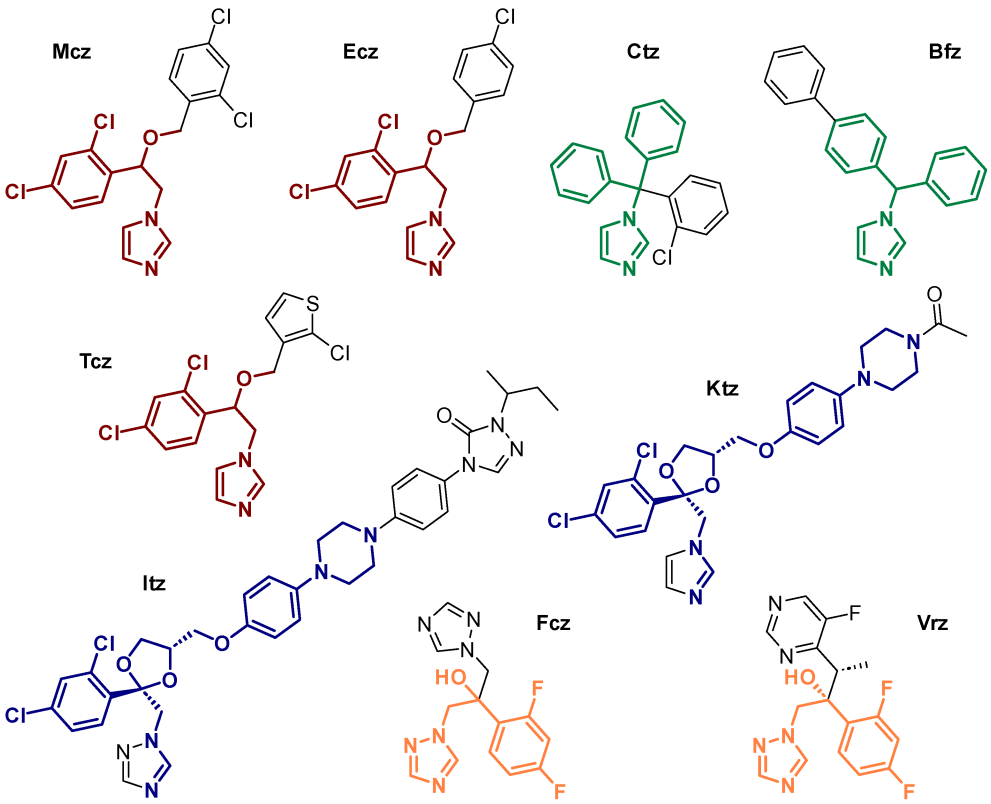

Scheme 1. Structure of selected examples of antifungal azoles (AAs): miconazole (Mcz), econazole (Ecz), tioconazole (Tcz), clotrimazole (Ctz), bifonazole (Bfz), ketoconazole (Ktz), itraconazole (Itz), fluconazole (Fcz) and voriconazole (Vrz), with emphasized structural similarities within the same family of AAs.

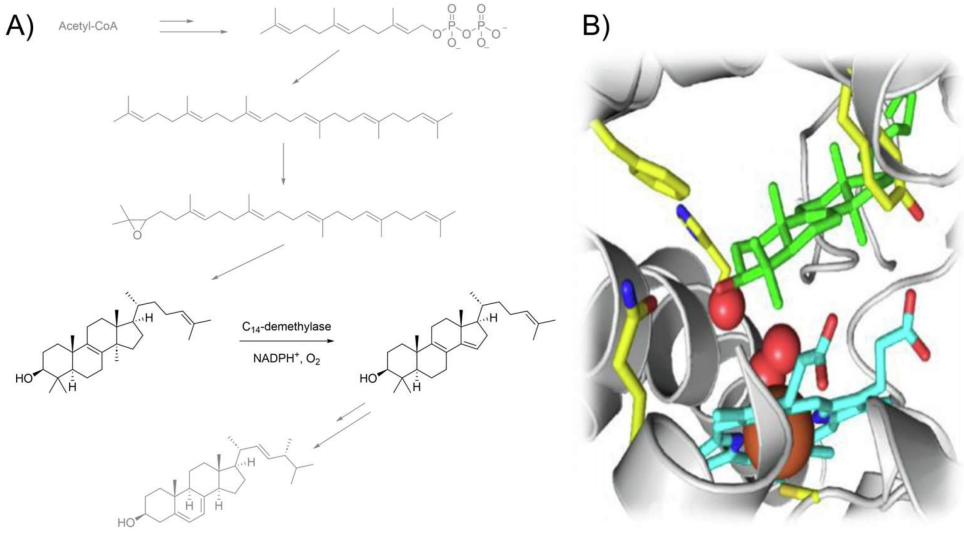

Figure 1. (**A**) Fungal ergosterol biosynthesis with lanosterol demethylation highlighted. (**B**) Schematic diagram of CYP51 catalytic site: lanosterol (green), heme (cyan), iron (orange).

Limiting AAs to their fungicidal properties would be shortsighted. Indeed, their ability to interact with CYP51 allows the inhibition of sterol biosynthesis in other organisms as well. In particular, activity against *T. cruzi*, the protozoan

parasite causing the Chaga's disease, and certain *Leshmania* species were reported, as these organisms share a similar ergosterol pathway compared to fungi [12][13].

AAs have shown their potential against prokaryotic pathogens too, as they have been known for a few decades to exhibit antibacterial activity [14][15]. In this case, the drug mechanism slightly differs from the one observed in fungal and protozoan species. Indeed, the AA probably binds the iron heme porphyrin of a bacterial deoxygenase called flavohemoglobin (**Figure 2**), preventing the conversion of nitrogen monoxide into nitrate by occupying the coordination site. The inability to expel NO molecules renders the bacterial organism vulnerable to NO-mediated damage induced, e.g., by host immune cells [16]. New evidence toward this mode of action was recently afforded by computational methods analyzing more than one hundred AAs and some of their close derivatives [17].

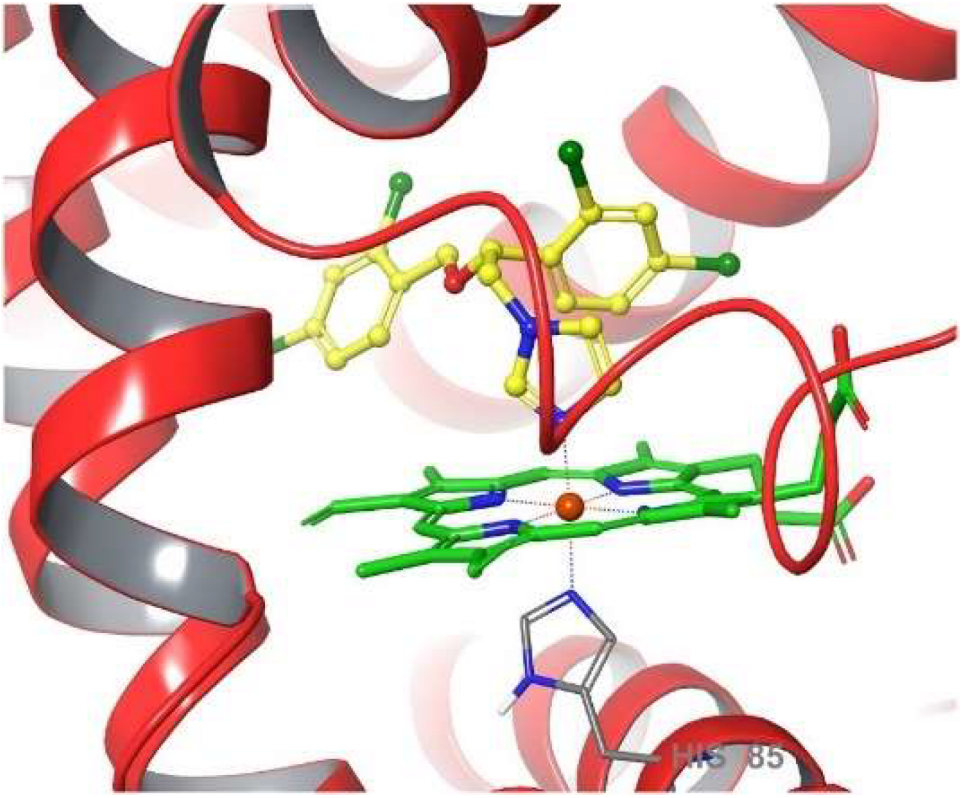

Figure 2. Schematic diagram of *R. eutropha* flavohemoglobin catalytic site with bound miconazole shown in yellow.

Finally, certain AAs have been studied for their anticancer properties, beginning with the investigation of ketoconazole (Ktz) as an androgen blocker through the inhibition of CYP17A1 enzyme for the treatment of prostate cancer [18]. Later, the cytotoxicity of miconazole (Mcz), econazole (Ecz), clotrimazole (Ctz) and itraconazole (Itz) was assessed in several publications, and proven to occur by various mechanisms of action including Ca^{2+} depletion, cell cycle arrest, glycolysis disturbance and the inhibition of the Hedgehog pathway [19]. The latter effect is especially recurrent in the case of Itz [20]. Other AAs, namely bifonazole (Bfz) [21] and tioconazole (Tcz) [22], have been scarcely analyzed for antitumoral purposes, while fluconazole (Fcz) and voriconazole (Vrz) yielded poor results in this medical application [23].

The potential combination of anticancer and antimicrobial activity in a single molecule obviously presents some advantages, considering, e.g., the necessity of prophylactic antifungal therapy in the case of immunocompromised patients who undergo certain transplants or chemotherapeutic treatments [24]. Infections caused by *Candida* sp. in hospitals have to be emphasized as well, because they remain a serious danger during prolonged antibiotic therapies, while multidrug treatments always carry the risk of undesired drug–drug interactions [25]. Furthermore, successfully extending the use of approved drugs outside of their original prescription constitutes a considerable gain of time and financial resources [26]. However, the repurposing of antimicrobial drugs as anticancer agents goes against the current measures preventing antibiotics misuse. It was indeed reported that such treatments promoted AMR in late stage cancer patients, threatening the health of other immunocompromised people [27].

Despite the above optimistic considerations about AAs, they are by no means new drugs and thus fail to answer the need for novel therapeutic agents. However, their Lewis basicity allows coordination to a metal center, as evidenced by their mechanisms of action. Metal complexation of well-established drugs constitutes a promising strategy to overcome loss of medication sensitivity and induced resistance [28]. Apart from the important biological activity of the metal ions, administrated in the form of approved metallodrugs [29][30][31][32][33], organometallic chemistry allows wider diversity in the design of medically relevant molecules, notably through higher number of possible geometries, redox features, non-covalent bonding and catalytic properties [29]. Moreover, the coordinated derivatives of biologically active ligands have been known to show synergistic effect with certain metal cores. This phenomenon, often referred to as ‘metal-drug synergism’ (MDS), can be explained by both an increase in drug activity, due to stabilization via complexation, leading to longer residence time, and a decrease in the metal toxicity, thanks to limited availability for undesired reactions compared, e.g., to the free hydrated ion [34]. In some cases, metal ions can regulate the activity of an organic drug or vice versa without requiring the intake of the corresponding metallodrug. Such examples concerning AAs are manifold in the literature [35][36][37][38][39][40][41][42][43][44][45][46][47].

2. Coordination Compounds of the Mcz Family of AAs

Developed by Janssen in 1968, Mcz entered the market as a topical antifungal agent in 1971. As the first synthesized and approved medically relevant AA, Mcz marked the advent of the first generation of these compounds. Simultaneously, Ecz was patented by the same company and a few years later, Tcz was designed by Pfizer [48]. Structurally speaking, these AAs are closely related to one another, as they all feature a metal-coordinating imidazole (imz), a dichlorophenyl ring and an etheric oxygen linked by an ethyl scaffold (Scheme 1). They differ from each other by the ether group bearing an aryl- or heteroarylmethyl moiety. As the predecessor of all AAs, Mcz remains the most investigated one in the field of coordination chemistry. Surprisingly, Tcz holds second place, despite Ecz displaying almost the same structure as Mcz.

The first study attempting to coordinate AAs from the Mcz family to a metal center was reported by Davis et al. in 1998. The authors described the synthesis of two square planar Ir(I) complexes bearing an *N*-heterocyclic carbene (NHC) derivative of Mcz and Ecz (**1** and **2**, respectively, Scheme 2). Crystals of **2** suitable for X-ray measurements were successfully grown, which helped deducing the structure of the Mcz analog, along with NMR spectroscopy

measurements. The reasoning behind this work was the production of biologically relevant organometallic NHCs known to be involved in the metabolism of vitamin B1. However, no further biological investigations were carried out [49].

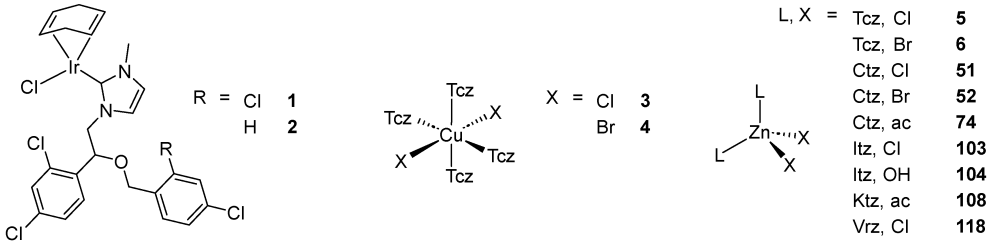

(**A**)

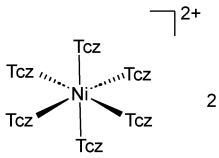

A = Cl **7**
Br **8**

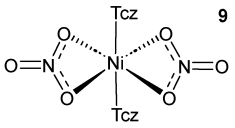

9

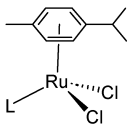

L = Mcz **10**
Tcz **13**
Ctz **37**
Ktz **94**

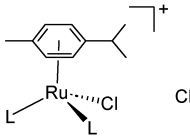

L = Mcz **11**
Tcz **14**
Ctz **46**

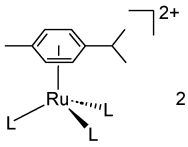

L = Mcz **12**
Tcz **15**
Ctz **47**

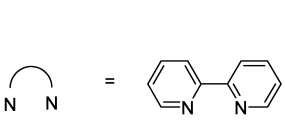

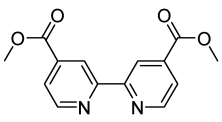

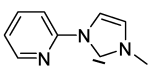

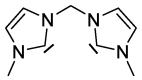

M, L, A = Mn, Mcz, PF_6 **16**
Mn, Ctz, PF_6 **55**
Mn, Ctz, OTf **56**
Re, Ctz, OTf **57**
Re, Ctz, PF_6 **63**
Mn, Ktz, PF_6 **100**

Mn, Mcz, PF_6 **17**
Mn, Ktz, PF_6 **101**

Mn, Ctz, OTf **58**

Mn, Ctz, OTf **59**

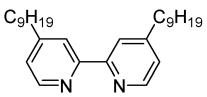

M, L, A = Mn, Ctz, OTf **60**

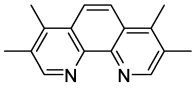

Re, Ctz, PF_6 **61**
Re, Ktz, PF_6 **102**

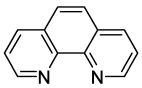

Re, Ctz, PF_6 **62**

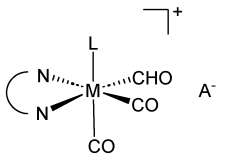

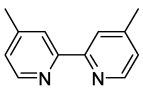

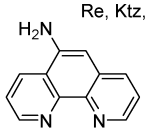

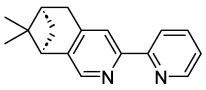

M, L, A = Re, Ctz, PF_6 **64**

Re, Ctz, PF_6 **65**

Re, Ctz, OTf **66**

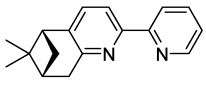

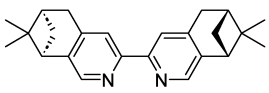

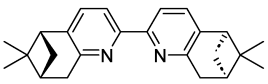

M, L, A = Re, Ctz, OTf **67**

Re, Ctz, OTf **68**

Re, Ctz, OTf **69**

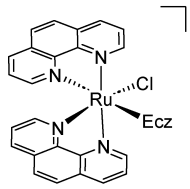

18

Cl⁻

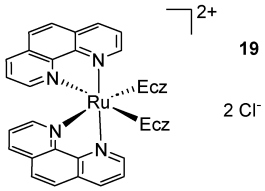

19

2 Cl⁻

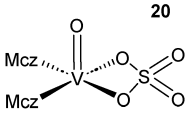

20

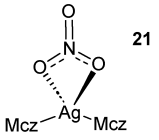

21

L, A = Mcz, ClO_4 **22**
Mcz, BF_4 **23**
Mcz, SbF_6 **24**
Ctz, NO_3 **70**
Itz, NO_3 **105**

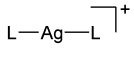

L = Ecz **25**
Tcz **26**
Ctz **29**
Vrz **133**

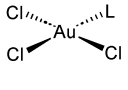

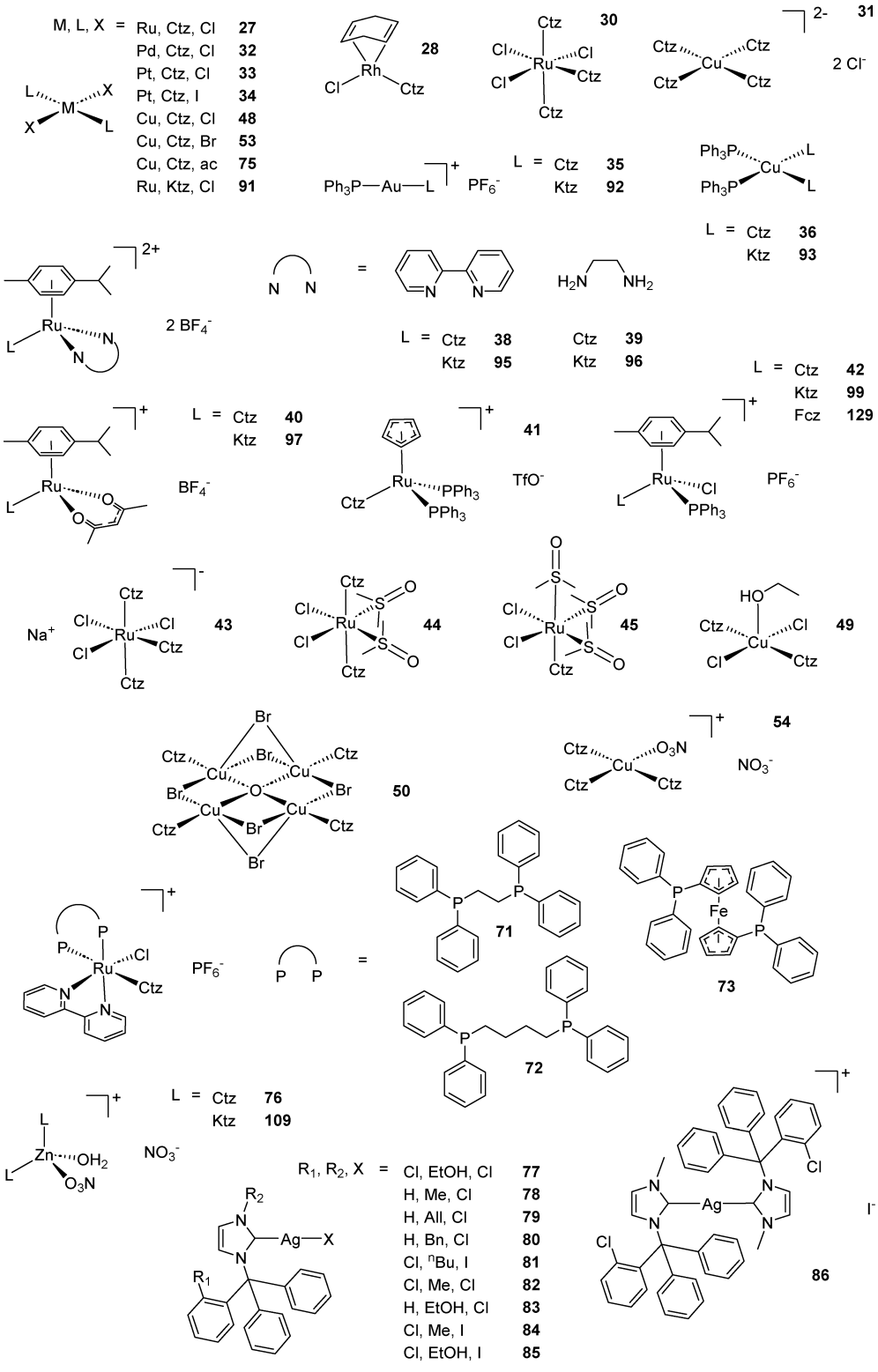
M, L, X =
Ru, Ctz, Cl 27
Pd, Ctz, Cl 32
Pt, Ctz, Cl 33
Pt, Ctz, I 34
Cu, Ctz, Cl 48
Cu, Ctz, Br 53
Cu, Ctz, ac 75
Ru, Ktz, Cl 91
28
30
31
2 Cl-
L = Ctz 35
Ktz 92
L = Ctz 36
Ktz 93
2 BF4-
L = Ctz 38
Ktz 95
Ctz 39
Ktz 96
L = Ctz 42
Ktz 99
Fcz 129
L = Ctz 40
Ktz 97
BF4-
41
TfO-
PF6-
Na+
43
44
45
49
50
54
NO3-
71
72
73
PF6-
L = Ctz 76
Ktz 109
NO3-
R1, R2, X = Cl, EtOH, Cl 77
H, Me, Cl 78
H, All, Cl 79
H, Bn, Cl 80
Cl, nBu, I 81
Cl, Me, Cl 82
H, EtOH, Cl 83
Cl, Me, I 84
Cl, EtOH, I 85
86
I-

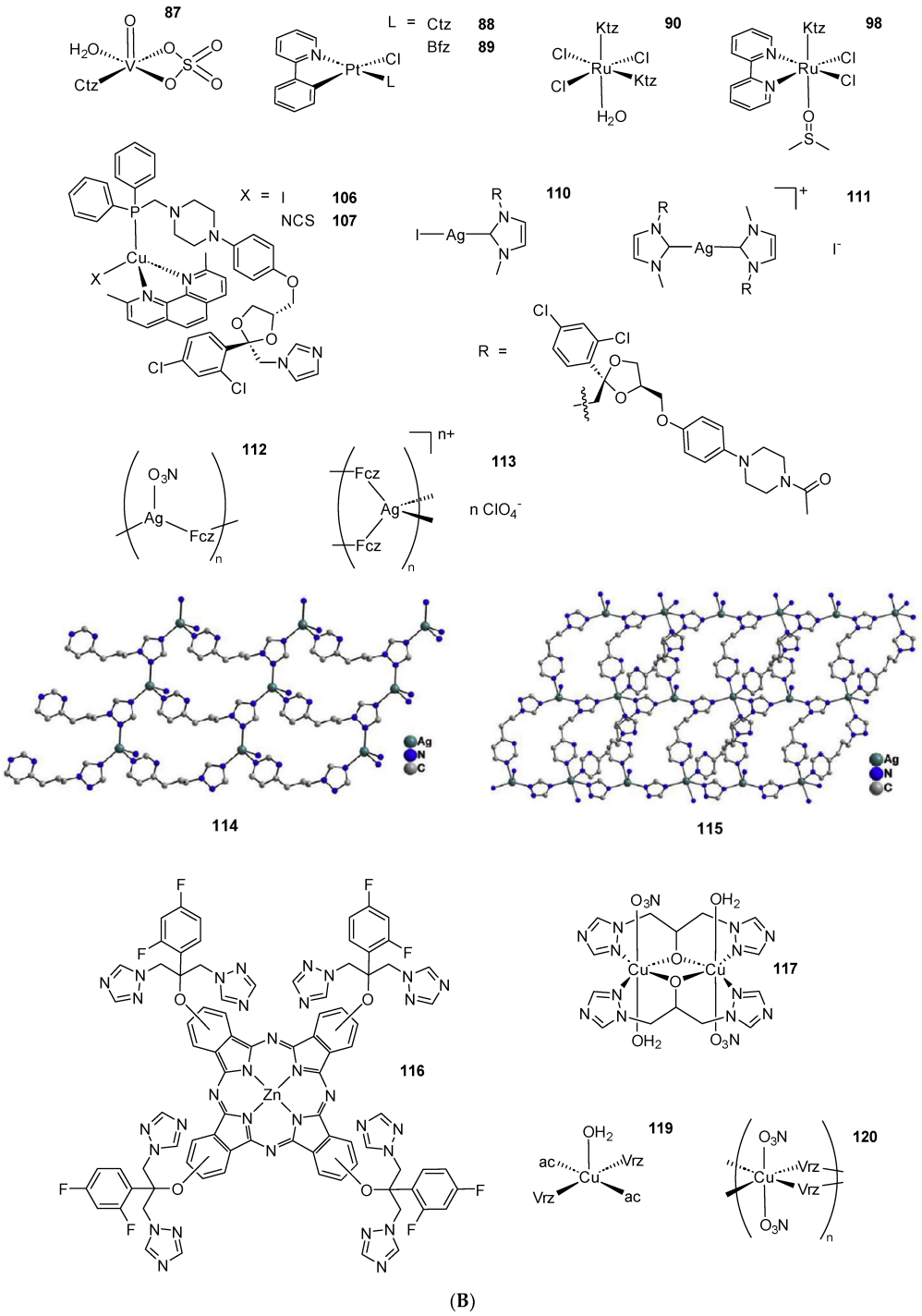
87
L = Ctz 88
Bfz 89
90
98
X = I 106
NCS 107
110
111
R =
112
113
n ClO4-
114
115
116
117
119
120
(B)

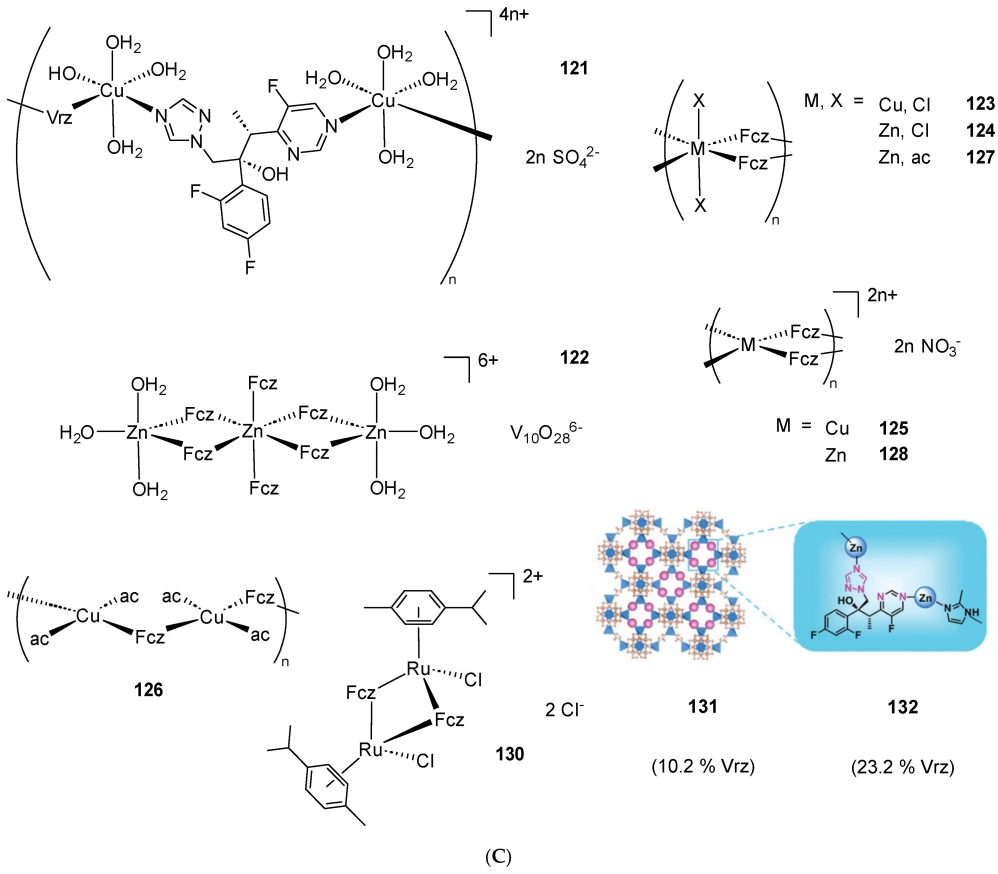

Scheme 2. (**A**) List of selected complexes discussed in this work (unless otherwise drawn, the coordination with AA ligands always occurs via the *N*3 atom of the imz ring or the *N*4 atom of the triazole ring); (**B**) the schematic view of the 2D layered structure of compounds **114** and **115** were obtained with permission; (**C**) the schematic representation of compounds **131** and **132** were obtained with permission.

More than one decade later, Abd El-Halim et al. published seven new aqua chloro complexes of Mcz with a Co(II), Cr(III), Cu(II), Fe(III), Mn(II), Ni(II) or Zn(II) metallic core and tested them in vitro against several fungi and bacteria strains [50]. The authors supported the proposed structures by elemental and thermal analysis, IR spectroscopy, magnetic moment and molar conductance determination. However, these data constitute hardly convincing evidence, due to their indirect nature and the confusing deduction toward the formation of so-called chelates. Four species of fungi (*A. fumigatus*, *C. albicans*, *P. italicum*, *S. racemosum*) and four species of bacteria (*B. subtilis*, *E. coli*, *P. aeruginosa*, *S. aureus*) were selected to perform the biological experiments. Globally, most complexes showed similar or slightly better growth inhibition than the free AA. Exceptions are *C. albicans* and *P. aeruginosa*, against which almost no compound displayed the same activity as Mcz. However, the best improvements in growth inhibition were provided by Fe(III) and Ni(II) complexes against *B. subtilis* and by the Zn(II) complex against *E. coli* [50]. Following the same protocol, the authors published a similar study concerning Tcz. In this case, the increase in activity through complexation of the drug was more striking. Notably, promising results were given by Cr(III), Fe(III) and Mn(II) complexes against *A. fumigatus*, by all seven complexes against *C. albicans*, by Cr(III) and Mn(II) complexes against *P. italicum*, by Cr(III) and Cu(II) complexes against *S. aureus* and by all complexes against *B. subtilis* [51].

This work was criticized by Barba-Behrens and coworkers for an abusive usage of the word ‘chelate’ and a lack of spectroscopic data in support of the proposed molecular geometries. By contrast, the group of Barba-Behrens synthesized a similar library of Tcz complexes possessing a Cd(II), Co(II), Cu(II) or Zn(II) metal center and provided strong evidence for the proposed structures by means of NMR, IR and UV-Vis-NIR spectroscopy, as well as elemental analysis, molar conductivity and magnetic susceptibility measurements. Furthermore, the crystal structures of **3**–**6** (Scheme 2) were elucidated. Following characterization, the compounds were tested against three cancer cell lines (HCT15, MCF7 and HeLa). No or low activity of the complexes was observed against the two last cell lines, apart from a mediocre IC_{50} value of 13.542 µg/mL for **6** on HeLa. Against HCT15 cells, four complexes showed similar activity compared to cisplatin, but only **3**, displaying an IC_{50} value of 3.10 µg/mL (6.78 µM wAA), was more active than this reference drug. In comparison, Tcz was not active against any of the three cell lines [52]. The same group expanded their series of Tcz derivatives by reporting the synthesis and cytotoxicity of eight new Ni(II), Pd(II) and Pt(II) complexes featuring this AA. These compounds were confirmed by NMR, IR, UV-Vis-NIR spectroscopy, ESI-MS, elemental and molar conductivity analysis. Additionally, crystals suitable for X-ray diffraction of **7** and **8** (Scheme 2) were successfully grown. The species were tested against the HCT15, HeLa, MCF7 and PC3 cell lines. Considering that Tcz did not show any measurable activity, the results revealed encouraging IC_{50} values below 100 µM.

In 2013, Gasser and coworkers showed the importance of careful interpretation of the biological data of piano stool Ru(II) complexes possessing a coordinated monodentate drug. A considerable number of these compounds displayed very similar IC_{50} values against HeLa and L6 cell lines compared to an equimolar mixture of the free drug and the corresponding complex bearing a DMSO molecule instead of the medically relevant ligand. Further NMR analysis concluded that dissociation of the drug was occurring in DMSO-d6, questioning the relevance of data obtained for certain coordination compounds which are often stored in DMSO for biological purposes. Among all three AA complexes considered in this study, an Mcz derivative (**10**, Scheme 2) showed such decomposition, but still revealed better activity than the free AA. Moreover, the authors tested this compound against *T. Cruzi*. The slight differences obtained between the IC_{50} value of **10** and an equimolar mixture of the corresponding DMSO complex with the uncoordinated AA emphasized the partial nature of the dissociation [53]. Turel and coworkers synthesized the same Mcz complex **10**, along with the corresponding compounds in which one or two chlorides were substituted by the same AA ligand (**11** and **12**, respectively, Scheme 2), as well as all the Tcz (**13**–**15**, Scheme 2) and Ctz analogs. The resulting nine complexes were confirmed by NMR, UV-Vis, IR and HRMS analysis and, in particular, X-ray crystallography of **13**, which, at the time, was the first reported structure of a Tcz coordination compound (**Figure 3**). All complexes were tested against *C. lunata* and showed lower growth rate inhibition than the free AA. Interestingly, the antifungal potency of the compounds inversely correlated with the number of AA ligands. In addition, **10**–**12** were tested against the worm *S. mansoni*, but lethal toxicity toward this parasite appeared only at concentrations of 100 µg/mL [54].

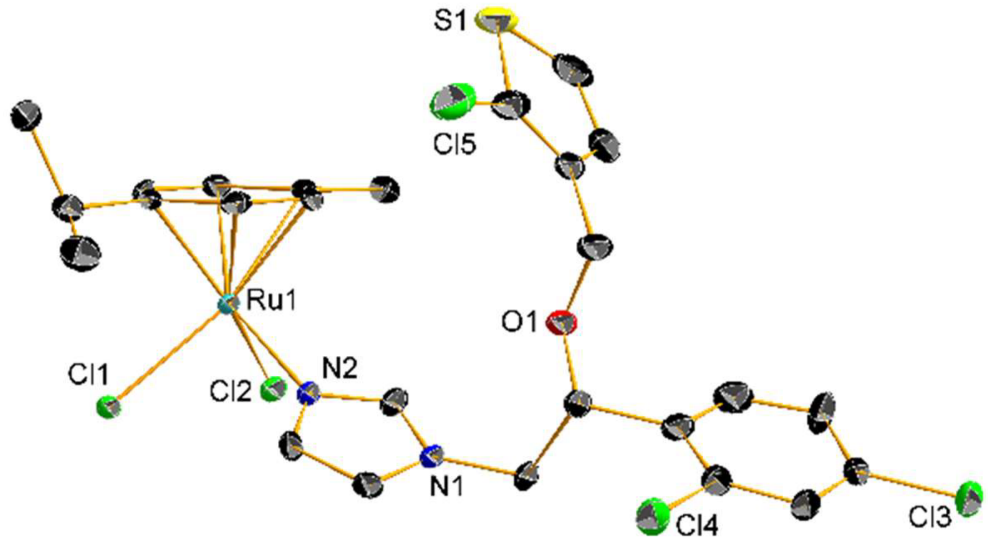

Figure 3. Crystal structure of **13** with thermal ellipsoids drawn at the 30% probability level and hydrogen atoms omitted for clarity.

Simpson et al. reported five new [2+1] *fac*-Mn(I) tricarbonyl complexes bearing an AA ligand and investigated their antimicrobial activity. The resulting species featured three carbonyl moieties, a monodentate AA ligand and a 2,2′-bipyridine (bpy) bidentate ligand derivative. These structures were confirmed by NMR, IR spectroscopy, as well as ESI-MS and DFT calculations. The compounds, among which two Mcz derivatives (**16** and **17**, Scheme 2), were tested against a series of four G+ bacteria (*S. aureus*, *S. epidermidis*, *E. faekalis*, *E. faecium*), four G− bacteria (*E. coli*, *P. aeruginosa*, *Y. pseudotuberculosa*, *Y. pestis*) and two kinetoplastids (*L. major*, *T. brucei*).

The same year, Karaoun and Renfrew investigated the cytotoxic and luminescent properties of two Ru(II) Ecz complexes (**18** and **19**, Scheme 2). The compounds were characterized by NMR, UV-Vis and fluorescence spectroscopy, as well as mass spectrometry and elemental analysis. Interestingly, UV-Vis and ESI-MS analysis revealed that in the dark, an aqueous solution of **18** undergoes complete substitution of the chloride ligand by water within 24 h, inducing a blue shift in the absorbance spectrum. Conversely, **19** only showed the analogous behavior upon irradiation with green light, which lead to substitution of one Mcz, producing phosphorescence, as well as the same aqua complex and the free AA. The luminescent phenomenon and the photochemical decomposition were proposed to occur competitively both from the ^{3}MLCT excited state, resulting in a turn-off phosphorescence response. With such properties, **19** was recognized as a potential photosensitizer for photodynamic therapy, and was thus tested on four cancer cell lines (MCF7, LNCaP, PC3 and DLD1), along with **18** and Ecz nitrate. The cytotoxicity of **19** remained relatively high in the dark, even exceeding that of the free AA occasionally. However, **18** and **19** were found to be almost equally active when irradiated, with IC_{50} values ranging from 0.4 µM to 2.85 µM (5.70 µM wAA). The authors concluded that the potency of these molecules probably originates from the production of their aqua derivative, although the latter globally displayed lower efficiency, possibly because of poor cellular uptake [55].

No other coordination compound from this family of AAs was then reported until 2020, when Aziz et al. investigated the ability of three Cr(III) complexes, one of which designed with a Mcz ligand, to bind the insulin receptor for antidiabetic purposes. This work was based on combination of theoretical data furnished by the authors through spectra simulations, DFT calculations and molecular docking studies with experimental data in the form of IR, UV-Vis spectroscopy, mass spectrometry, TGA, molar conductivity measurements and DNA binding affinity tests. The obtained correlations, varying from moderate to excellent, provided evidence for the proposed structures. The potential of the complexes to bind the insulin receptor was assessed by calf thymus DNA (ctDNA) titration with each compound. The resulting hyperchromism observed by UV-Vis spectroscopy yielded a binding constant (K_b) of 10^6 M^{-1} for the Mcz derivative. Meanwhile, molecular docking calculations revealed the high affinity of this compound for the insulin receptor [56]. Adopting a similar dual theoretical–experimental approach, Hussien and coworkers reported the synthesis of three V(IV) inorganic compounds, among which **20** (Scheme 2), as well as their DNA binding ability and their cytotoxicity in vitro. Titration of ctDNA with **20** resulted in spectroscopic hypochromism. From this experiment, the authors deduced the affinity of the complex with DNA, supported by DFT calculations, and hypothesized an intercalation mechanism. However, the anticancer tests carried out against HepG2 and MCF7 cell lines showed IC_{50} values of 5.27 µM (10.5 µM wAA) and 2.98 µM (5.96 µM wAA), respectively, which is lower than cisplatin in both cases (25.5 µM and 19.0 µM, respectively). No comparison with the activity of the free AA was reported [57].

Two Ag(I) Mcz complexes, namely **21** and **22** (Scheme 2), were studied by Ochocky and coworkers for their cytotoxicity. Crystals suitable for X-ray spectroscopy were obtained, and the resulting structures revealed distorted linear geometries (**Figure 4**A,B). Despite their similar molecular formula, these compounds exhibited notable structural differences, among which a N-Ag-N angle significantly lower than 180°, coplanarity of the two imz moieties and stronger interaction with the counterion in the case of **21**. The results suggested that **21** and **22** lie at extreme values within their group of analogs, considering the Ag-N and Ag-O bond lengths, as well as the N-Ag-N angle. In order to assess their anticancer properties, **21** and **22** were tested against HepG2 and non-tumoral Balb/c3T3 cell lines using four biochemical endpoints in order to determine their IC_{20} and IC_{50} values.

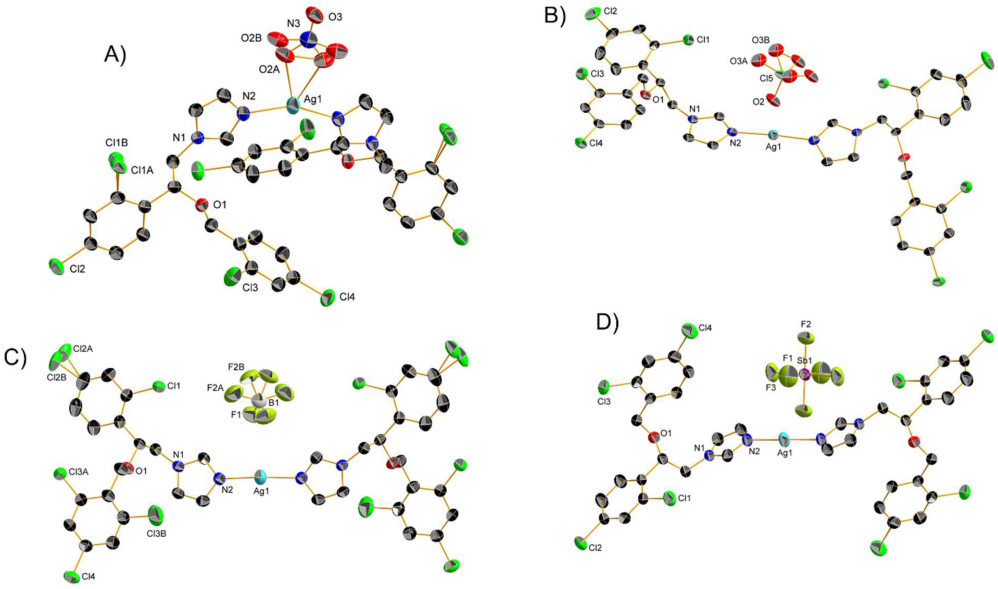

Figure 4. Crystal structures of (**A**) **21**, (**B**) **22**, (**C**) **23** and (**D**) **24** with thermal ellipsoids drawn at the 50% probability level and hydrogen atoms omitted for clarity.

The author complemented their study with two new similar coordination compounds bearing a BF_4^- and a SbF_6^- counterion (**23** and **24**, respectively, Scheme 2). As determined by X-ray crystallography (**Figure 4**C,D), the latter displayed linear geometry like their ClO_4^- analog **22** with an N-Ag-N angle of exactly 180° measured in the case of **24**. Moreover, **24** is the only compound of the series to possess an inversion center at the silver atom thanks to the peculiar relative position of the two Mcz ligands. Aware of the AA medicinal versatility, the authors decided to test the whole series of four complexes in vitro against G+ (*S. aureus*, *S.epidemnidis*, *M. luteus*, *B. subtilis*, *B. cereus*, *E. faecalis*) and G− bacteria (*S. typhimurium*, *E. coli*, *P. mirabilis*, *K. pneumoniae*, *P.aeruginosa*), as well as yeasts (*C. glabrata*, *C. albicans*, *C. parapsilosis*).

Stevanovic et al. published a recent study concerning AA coordination compounds of the Mcz family. In this work, an extensive biological investigation of seven square planar Au(III) trichloro complexes bearing an imz derivative ligand was carried out. Compounds **25** and **26** (Scheme 2) were characterized by NMR, UV-Vis and IR spectroscopy, as well as molar conductivity analysis. Additionally, crystals of **25** suitable for X-ray measurements were successfully grown. The authors first tested these compounds against different *Candida* strains (*C. albicans*, *C. parapsilosis*, *C. glabrata*, *C. krusei*, *C. auris*) and healthy MRC5 human cells. Namely, **26** showed a more than 20-fold improvement in activity against *C. krusei* compared to Tcz. The same compound exhibited submicromal MIC values against *C. albicans* and *C. parapsilosis*, but was relatively toxic toward healthy cells (IC_{50} value of 6.5 µM). Conversely, **25** showed a higher IC_{50} value against MRC5 cell line (26.3 µM) than any measured MIC value toward the yeasts. Against G+ (*S. aureus*, *S. aureus* MRSA) and G− (*E.coli*, *P. aeruginosa*) bacteria, the potency gap between the two complexes and their corresponding AA was even more striking. The best activity was found against *P. aeruginosa* and especially *S. aureus* MRSA, which is surprising, given the resistant nature of this strain. Furthermore, **25** and **26** showed the capacity to inhibit *P. aeruginosa* pyocyanin production. These two complexes were even active at lower concentration and revealed significantly better results when diluted from 20 µg/mL to 10 µg/mL. This interesting feature was used in a last assay combining *P. aeruginosa* with A549 cancer cells in which the two compounds decreased cell death by approximately 15% at a 5 µg/mL (7.3 µM) concentration of **25** and a 2.5 µg/mL (3.6 µM) concentration of **26** [58].

References

1. World Health Organization. WHO Report on Cancer: Setting Priorities, Investing Wisely and Providing Care for all; World Health Organization: Geneva, Switzerland, 2020.
2. O'Neill, J. Review on Antimicrobial Resistance: Tackling Drug-Resistant Infections Globally: Final Report and Recommendations; Wellcome Trust: London, UK, 2016; p. 80.
3. Plackett, B. Why big pharma has abandoned antibiotics. Nature 2020, 586, S50–S52.

4. World Health Organization. Ending the Neglect to Attain the Sustainable Development Goals: A Road Map for Neglected Tropical Diseases 2021–2030; World Health Organization: Geneva, Switzerland, 2021.
5. Yuzo, Y.; Yuri, A. Interaction of azole antifungal agents with cytochrome P-45014DM purified from Saccharomyces cerevisiae microsomes. Biochem. Pharmacol. 1987, 36, 229–235.
6. Yoshida, Y. Cytochrome P450 of Fungi: Primary Target for Azole Antifungal Agents. In Current Topics in Medical Mycology; McGinnis, M.R., Ed.; Springer: New York, NY, USA, 1988; pp. 388–418.
7. Aoyama, Y.; Yoshida, Y.; Sonoda, Y.; Sato, Y. Deformylation of 32-oxo-24,25-dihydrolanosterol by the purified cytochrome P-45014DM (lanosterol 14 α-demethylase) from yeast evidence confirming the intermediate step of lanosterol 14 α-demethylation. J. Biol. Chem. 1989, 264, 18502–18505.
8. Joseph-Horne, T.; Hollomon, D.W. Molecular mechanisms of azole resistance in fungi. FEMS Microbiol. Lett. 1997, 149, 141–149.
9. White Theodore, C.; Marr Kieren, A.; Bowden Raleigh, A. Clinical, Cellular, and Molecular Factors That Contribute to Antifungal Drug Resistance. Clin. Microbiol. Rev. 1998, 11, 382–402.
10. Mast, N.; Zheng, W.; Stout, C.D.; Pikuleva, I.A. Antifungal Azoles: Structural Insights into Undesired Tight Binding to Cholesterol-Metabolizing CYP46A1. Mol. Pharmacol. 2013, 84, 86.
11. Shafiei, M.; Peyton, L.; Hashemzadeh, M.; Foroumadi, A. History of the development of antifungal azoles: A review on structures, SAR, and mechanism of action. Bioorg. Chem. 2020, 104, 104240.
12. Musiol, R.; Kowalczyk, W. Azole Antimycotics—A Highway to New Drugs or a Dead End? Curr. Med. Chem. 2012, 19, 1378–1388.
13. Choi, J.Y.; Podust, L.M.; Roush, W.R. Drug Strategies Targeting CYP51 in Neglected Tropical Diseases. Chem. Rev. 2014, 114, 11242–11271.
14. Fromtling, R.A. Overview of medically important antifungal azole derivatives. Clin. Microbiol. Rev. 1988, 1, 187–217.
15. Alsterholm, M.; Karami, N.; Faergemann, J. Antimicrobial activity of topical skin pharmaceuticals—An in vitro study. Acta Derm. Venereol. 2010, 90, 239–245.
16. Helmick Ryan, A.; Fletcher Arin, E.; Gardner Anne, M.; Gessner Christopher, R.; Hvitved Angela, N.; Gustin Michael, C.; Gardner Paul, R. Imidazole Antibiotics Inhibit the Nitric Oxide Dioxygenase Function of Microbial Flavohemoglobin. Antimicrob. Agents Chemother. 2005, 49, 1837–1843.
17. Sari, S.; Avci, A.; Koçak, E.; Kart, D.; Sabuncuoğlu, S.; Doğan, İ.S.; Özdemir, Z.; Bozbey, İ.; Karakurt, A.; Saraç, S.; et al. Antibacterial azole derivatives: Antibacterial activity, cytotoxicity, and

in silico mechanistic studies. Drug Dev. Res. 2020, 81, 1026–1036.

18. Amery, W.K.; De Coster, R.; Caers, I. Ketoconazole: From an antimycotic to a drug for prostate cancer. Drug Dev. Res. 1986, 8, 299–307.
19. Weng, N.; Zhang, Z.; Tan, Y.; Zhang, X.; Wei, X.; Zhu, Q. Repurposing antifungal drugs for cancer therapy. J. Adv. Res. 2022, 48, 259–273.
20. Tsubamoto, H.; Ueda, T.; Inoue, K.; Sakata, K.; Shibahara, H.; Sonoda, T. Repurposing itraconazole as an anticancer agent (Review). Oncol. Lett. 2017, 14, 1240–1246.
21. Penso, J.; Beitner, R. Clotrimazole and bifonazole detach hexokinase from mitochondria of melanoma cells. Eur. J. Pharmacol. 1998, 342, 113–117.
22. Sebastian, J.; Rathinasamy, K. Cytotoxic mechanism of tioconazole involves cell cycle arrest at mitosis through inhibition of microtubule assembly. Cytotechnology 2022, 74, 141–162.
23. Gupta, A.; Unadkat, J.D.; Mao, Q. Interactions of azole antifungal agents with the human breast cancer resistance protein (BCRP). J. Pharm. Sci. 2007, 96, 3226–3235.
24. Weinstein, R.A.; Rex, J.H.; Sobel, J.D. Prophylactic Antifungal Therapy in the Intensive Care Unit. Clin. Infect. Dis. 2001, 32, 1191–1200.
25. Azevedo, M.M.; Teixeira-Santos, R.; Silva, A.P.; Cruz, L.; Ricardo, E.; Pina-Vaz, C.; Rodrigues, A.G. The effect of antibacterial and non-antibacterial compounds alone or associated with antifugals upon fungi. Front. Microbiol. 2015, 6, 669.
26. Pushpakom, S.; Iorio, F.; Eyers, P.A.; Escott, K.J.; Hopper, S.; Wells, A.; Doig, A.; Guilliams, T.; Latimer, J.; McNamee, C.; et al. Drug repurposing: Progress, challenges and recommendations. Nat. Rev. Drug Discov. 2019, 18, 41–58.
27. Mamak, T.; Hadiseh, H.; Shirin, F.; Masoud, P.; Mohammadreza, S.; Mahsa, A. Antibiotic Treatment in End Stage Cancer Patients; Advantages and Disadvantages. Cancer Inform. 2023, 22, 11769351231161476.
28. Chellan, P.; Sadler, P.J. Enhancing the Activity of Drugs by Conjugation to Organometallic Fragments. Chem. Eur. J. 2020, 26, 8676–8688.
29. Gasser, G.; Metzler-Nolte, N. The potential of organometallic complexes in medicinal chemistry. Curr. Opin. Chem. Biol. 2012, 16, 84–91.
30. Barry, N.P.E.; Sadler, P.J. Exploration of the medical periodic table: Towards new targets. Chem. Commun. 2013, 49, 5106–5131.
31. Mjos, K.D.; Orvig, C. Metallodrugs in Medicinal Inorganic Chemistry. Chem. Rev. 2014, 114, 4540–4563.

32. Anthony, E.J.; Bolitho, E.M.; Bridgewater, H.E.; Carter, O.W.L.; Donnelly, J.M.; Imberti, C.; Lant, E.C.; Lermyte, F.; Needham, R.J.; Palau, M.; et al. Metallodrugs are unique: Opportunities and challenges of discovery and development. Chem. Sci. 2020, 11, 12888–12917.
33. Ferraro, G.; Merlino, A. Metallodrugs: Mechanisms of Action, Molecular Targets and Biological Activity. Int. J. Mol. Sci. 2022, 23, 3504.
34. Farrell, N. Transition Metal Complexes as Drugs and Chemotherapeutic Agents; Springer: Berlin/Heidelberg, Germany, 1989; Volume 11.
35. Sarachek, A.; Henderson, L.A. Modification of responses of Candida albicans to cisplatin by membrane damaging antimycotic agents. Mycoses 1991, 34, 177–182.
36. Minn, Y.; Brummer, E.; Stevens, D.A. Effect of iron on fluconazole activity against Candida albicans in presence of human serum or monocyte-derived macrophages. Mycopathologia 1997, 138, 29–35.
37. Uthman, A.; Rezaie, S.; Dockal, M.; Ban, J.; Söltz-Szöts, J.; Tschachler, E. Fluconazole downregulates metallothionein expression and increases copper cytotoxicity in Microsporum canis. Biochem. Biophys. Res. Commun. 2002, 299, 688–692.
38. Eshwika, A.; Coyle, B.; Devereux, M.; McCann, M.; Kavanagh, K. Metal complexes of 1,10-phenanthroline-5,6-dione alter the susceptibility of the yeast Candida albicans to Amphotericin B and Miconazole. BioMetals 2004, 17, 415–422.
39. Oyama, T.M.; Oyama, T.B.; Oyama, K.; Sakanashi, Y.; Morimoto, M.; Matsui, H.; Oyama, Y. Clotrimazole, an antifungal drug possessing diverse actions, increases membrane permeation of cadmium in rat thymocytes. Toxicol. Vitr. 2007, 21, 1505–1512.
40. Oyama, Y.; Matsui, H.; Morimoto, M.; Sakanashi, Y.; Nishimura, Y.; Ishida, S.; Okano, Y. Synergic cytotoxic action induced by simultaneous application of zinc and clotrimazole in rat thymocytes. Toxicol. Lett. 2007, 171, 138–145.
41. Matsui, H.; Sakanashi, Y.; Oyama, T.M.; Oyama, Y.; Yokota, S.-i.; Ishida, S.; Okano, Y.; Oyama, T.B.; Nishimura, Y. Imidazole antifungals, but not triazole antifungals, increase membrane Zn2+ permeability in rat thymocytes: Possible contribution to their cytotoxicity. Toxicology 2008, 248, 142–150.
42. Kinazaki, A.; Sakanashi, Y.; Oyama, T.M.; Shibagaki, H.; Yamashita, K.; Hashimoto, E.; Nishimura, Y.; Ishida, S.; Okano, Y.; Oyama, Y. Micromolar Zn2+ potentiates the cytotoxic action of submicromolar econazole in rat thymocytes: Possible disturbance of intracellular Ca2+ and Zn2+ homeostasis. Toxicol. Vitr. 2009, 23, 610–616.
43. Hunsaker, E.W.; Franz, K.J. Copper potentiates azole antifungal activity in a way that does not involve complex formation. Dalton Trans. 2019, 48, 9654–9662.

44. Hunsaker, E.W.; Franz, K.J. Candida albicans reprioritizes metal handling during fluconazole stress. Metallomics 2019, 11, 2020–2032.
45. da Silva Hellwig, A.H.; Pagani, D.M.; Rios, I.d.S.; Ribeiro, A.C.; Zanette, R.A.; Scroferneker, M.L. Influence of iron on growth and on susceptibility to itraconazole in Sporothrix spp. Med. Mycol. 2021, 59, 400–403.
46. Gaspar-Cordeiro, A.; Amaral, C.; Pobre, V.; Antunes, W.; Petronilho, A.; Paixão, P.; Matos, A.P.; Pimentel, C. Copper Acts Synergistically with Fluconazole in Candida glabrata by Compromising Drug Efflux, Sterol Metabolism, and Zinc Homeostasis. bioRxiv 2021, 13, 920574.
47. Hunsaker, E.W.; Yu, C.-H.A.; Franz, K.J. Copper Availability Influences the Transcriptomic Response of Candida albicans to Fluconazole Stress. G3 Genes Genomes Genet. 2021, 11, jkab065.
48. Alapi, E.M.; Fischer, J. Table of Selected Analogue Classes. In Analogue-Based Drug Discovery; John Wiley & Sons: Hoboken, NJ, USA, 2006; pp. 441–552.
49. Davis, J.H.; Lake, C.M.; Bernard, M.A. Azolidene Carbenes Derived from Biologically Relevant Molecules. 1 Synthesis and Characterization of Iridium Complexes of Imidazolidene Ligands Based upon the Antifungal Drugs Econazole and Miconazole. Inorg. Chem. 1998, 37, 5412–5413.
50. Abd El-Halim, H.F.; Nour El-Dien, F.A.; Mohamed, G.G.; Mohamed, N.A. Synthesis, spectroscopic, thermal characterization, and antimicrobial activity of miconazole drug and its metal complexes. J. Therm. Anal. Calorim. 2012, 109, 883–892.
51. Abd El-Halim, H.F.; Nour El-Dien, F.A.; Mohamed, G.G.; Mohamed, N.A. Chelating behavior, thermal studies and biocidal efficiency of tioconazole and its complexes with some transition metal ions. J. Therm. Anal. Calorim. 2013, 111, 173–181.
52. Crisóstomo-Lucas, C.; García-Holley, P.; Hernández-Ortega, S.; Sánchez-Bartéz, F.; Gracia-Mora, I.; Barba-Behrens, N. Structural characterization and cytotoxic activity of tioconazole coordination compounds with cobalt(II), copper(II), zinc(II) and cadmium(II). Inorg. Chim. Acta 2015, 438, 245–254.
53. Patra, M.; Joshi, T.; Pierroz, V.; Ingram, K.; Kaiser, M.; Ferrari, S.; Spingler, B.; Keiser, J.; Gasser, G. DMSO-Mediated Ligand Dissociation: Renaissance for Biological Activity of N-Heterocyclic-Drug Candidates. Chem. Eur. J. 2013, 19, 14768–14772.
54. Kljun, J.; Scott, A.J.; Lanišnik Rižner, T.; Keiser, J.; Turel, I. Synthesis and Biological Evaluation of Organoruthenium Complexes with Azole Antifungal Agents. First Crystal Structure of a Tioconazole Metal Complex. Organometallics 2014, 33, 1594–1601.
55. Karaoun, N.; Renfrew, A.K. A luminescent ruthenium(ii) complex for light-triggered drug release and live cell imaging. Chem. Comm. 2015, 51, 14038–14041.

56. Aziz, S.G.; Elroby, S.A.; Jedidi, A.; Babgi, B.A.; Alshehri, N.S.; Hussien, M.A. Synthesis, characterization, computational study, DNA binding and molecular docking studies of chromium (III) drug-based complexes. J. Mol. Struct. 2020, 1215, 128283.
57. Basaleh, A.S.; Alomari, F.Y.; Sharfalddin, A.A.; Al-Radadi, N.S.; Domyati, D.; Hussien, M.A. Theoretical Investigation by DFT and Molecular Docking of Synthesized Oxidovanadium(IV)-Based Imidazole Drug Complexes as Promising Anticancer Agents. Molecules 2022, 27, 2796.
58. Stevanović, N.L.; Kljun, J.; Aleksic, I.; Bogojevic, S.S.; Milivojevic, D.; Veselinovic, A.; Turel, I.; Djuran, M.I.; Nikodinovic-Runic, J.; Glišić, B.Đ. Clinically used antifungal azoles as ligands for gold(iii) complexes: The influence of the Au(iii) ion on the antimicrobial activity of the complex. Dalton Trans. 2022, 51, 5322–5334.